

Proceedings of the Combustion Institute, Volume 29, 2002/pp. 000–000

## INHIBITION OF PREMIXED AND NON-PREMIXED FLAMES WITH FINE DROPLETS OF WATER AND SOLUTIONS

H. K. CHELLIAH,<sup>1</sup> A. K. LAZZARINI,<sup>1</sup> P. C. WANIGARATHNE,<sup>1</sup> AND G. T. LINTERIS<sup>2</sup>

<sup>1</sup>*Department of Mechanical and Aerospace Engineering  
University of Virginia*

*Charlottesville, VA 22904, USA*

<sup>2</sup>*Building and Fire Research Laboratory  
National Institute of Standards and Technology  
Gaithersburg, MD 20899, USA*

Inhibition/extinction of premixed and non-premixed methane/air flames with fine droplets of water and solutions containing several chemical agents has been investigated experimentally. While solutions allow delivery of much higher concentrations of chemical agent to the flame front than otherwise possible, the non-premixed flame extinction results indicate saturation (or condensation) of the agent at some effective temperature below the flame temperature. Based on the chemical additives considered, on a molar basis, the following order of effectiveness is observed:  $\text{KOH} > \text{NaCl} > \text{NaOH}$ . The inhibition of premixed flames by similar size droplets indicates insensitivity to NaOH mass fraction in the water. This insensitivity was related to the shorter residence time of the droplets ( $13 \mu\text{m}$  median diameter) through the premixed flame structure. Detailed comparison of the premixed and non-premixed flame inhibition/extinction with pure water droplets supports the importance of droplet residence time and optimum droplet size in controlling the interaction of droplets with the flame front.

### Introduction

Since the international ban on production of halon 1301 (because of its adverse effect on stratospheric ozone), application of fine water droplets as an effective fire suppressant has received considerable attention. Fire suppression by fine water droplets is attributed to thermal effects associated with latent heat of vaporization [1], and recent laboratory studies [2] and parallel modeling efforts have established quantitative estimates of these thermal contributions [3,4]. Further enhancement of the fire suppression ability of fine water droplets through the use of chemical agents has recently received considerable attention [5,6] and is the main focus of the present investigation. Alkali metals have a strong chemical effect in flames, about an order of magnitude more than  $\text{CF}_3\text{Br}$ , and consequently are good candidates for addition to water sprays. Because of the low vapor pressure of these metals (for example partial pressure  $\sim 10^{-32}$  of NaOH at 298 K), they require application as a condensed phase, either as a fine powder or as a solution in fine water spray, to obtain any significant flame suppression.

In order to understand the suppression mechanisms and to optimize the performance of chemical agents added to water droplets, it is desired to conduct experiments which can be used as a database for detailed numerical modeling. Extensive tests of metal salts added to a hybrid diffusion-premixed flame were

conducted by Vanpee and Shirodkar [7], providing valuable data on the effectiveness of metals as flame inhibitors. However, their experiments are difficult to model because important experimental parameters were not provided (e.g., the equivalence ratio of partially premixed flames considered and the droplet sizes). Furthermore, their experiments were not conducted over a range of additive mole fractions, which, as described in this paper, is an important parameter. Experiments by Mitani and Niioaka [8] considered inhibition of premixed flames with ultrafine water droplets (less than  $2.4 \mu\text{m}$  mean diameter) containing NaOH and  $\text{NaHCO}_3$ , indicating a flame inhibition/extinction with addition of chemical agents. In particular, their slower  $\text{C}_2\text{H}_4/\text{O}_2/\text{N}_2$  premixed flame experiments (as opposed to faster  $\text{H}_2/\text{O}_2/\text{N}_2$  flames) showed distinct chemical inhibition effects, but the saturation effects due to condensation of metal vapors were not explored. Recent work by Zheng et al. [5] on counterflow premixed flames inhibited with water/NaCl fine droplets in fact show signs of saturation with increasing NaCl mass fraction in water. But the reported data on equivalence ratio versus flame extinction strain rate, at constant water mass addition, is not sufficient to extract meaningful information.

Motivated by the need to gain detailed understanding of the parameters important for water additives to be effective inhibitors in flames and to provide a database suitable for numerical models

currently being developed, we conducted the experiments described below. As will be demonstrated, droplet size, droplet residence time in the flame, and the saturation of active species produced by the chemical additive are key factors which must be controlled to obtain peak performance for the given time-temperature characteristics of an actual fire.

### Experimental Method

Two laboratory flame configurations were used, producing non-premixed and premixed methane/air flames. The burners were designed to be modular, so that the same water-generation and gas-supply systems could be used with either. The air was supplied by an oil-free shop compressor followed by a series of desiccant beds, and the fuel gas was methane (BOC grade 4.0, 99.99% purity). For the non-premixed flames, gas flows were measured by Teledyne Hastings-Raydist flow meters (factory calibrated with a reported accuracy of  $\pm 1\%$  of full-scale reading), and for the premixed flames, by Sierra model 860 mass flow controllers (calibrated with a Bios model 20 K piston flow meter so that their expanded relative uncertainty is 2%). For experiments involving water droplets, the metered dry air was saturated with water vapor before feeding to the burner [6]. The relative humidity was verified with a hygrometer (Testo 605-H1). (*Note:* Certain commercial equipment, instruments, or materials are identified in this paper to adequately specify the procedure. Such identification does not imply recommendation or endorsement by the National Institute of Standards and Technology, nor does it imply that the materials or equipment are necessarily the best available for the intended use.)

The droplet generation system used (Sono-Tek Model 8700-120) consisted of the ultrasonic nozzle and a broadband ultrasonic frequency generator. A syringe pump (Instech Model 2000) with a plastic 10 cc syringe fed water to the atomizer. The water mass flow rate at the nozzle exit was measured gravimetrically by carefully collecting the droplets on a collection cup. While the fraction of water fed to the atomizer which actually reached the nozzle exit was only about 70%, the operation of the droplet injection system was very consistent over the entire range of water and air flows of the tests. Near the atomizer tip, the droplet size distribution has been characterized by the manufacturer as a lognormal distribution, with a median diameter of about 18  $\mu\text{m}$  and a Sauter mean diameter of about 30  $\mu\text{m}$ . However, the actual droplet size distribution at the gas nozzle exit can deviate slightly because of settling of larger droplets in the vertical delivery tube. The associated shift in size distribution has been characterized using a phase Doppler particle analyzer, indicating a median diameter of about 13  $\mu\text{m}$  [6].

### Counterflow Burner

In the counterflow burner, a steady, planar, non-premixed flame was established in the mixing layer of the opposed methane and air streams. The fine water droplets were introduced with the airstream, which was first saturated with water vapor to eliminate evaporation of the droplets prior to their reaching the hot thermal mixing layer. The fuel and air nozzles (Pyrex glass) each have an area contraction ratio of 6.5 and an exit diameter of 1.5 cm and, at their exits, have nearly plug flow velocity profiles (verified previously through laser Doppler velocimetry measurements [9]). Co-flowing nitrogen streams on both the fuel and air sides helped to maintain a very stable planar flame disk. The nozzles were enclosed in a cylindrical burner chamber in which water cooling coils and air dilution of the postcombustion gases eliminate secondary flames. The nozzle tubes enter the chamber through vacuum fittings which permit easy adjustment of the nozzle separation distance ( $L$ ), which is typically set to 12 mm. A schematic and a detailed description of this burner can be found in Ref. [6].

In the non-premixed flame experiments, the water mass flow rate was fixed, and the air and methane flows were increased together until the flame was extinguished. The fuel and air flows were adjusted so as to balance their momentum; that is,  $(\rho v^2)_{\text{air}} = (\rho v^2)_{\text{CH}_4}$ , where  $\rho$  is the density and  $v$  is the axial velocity. Knowing the nozzle separation distance, the global flow strain rate at extinction is defined by  $a_{\text{ext}} = 4|v_{\text{air}}|/L$ , providing a suitable parameter that describes the non-premixed flame extinction condition [10]. The total water (or solution) droplet mass fraction in the air + saturated water vapor stream is defined here as  $Y_0$ , while the mass fraction of the additive (i.e., NaOH, KOH, NaCl, or  $\text{FeCl}_2$ ) is defined as  $y_{\text{add}}$ . In experiments, variation of  $a_{\text{ext}}$  with  $Y_0$  as well as  $y_{\text{add}}$  were measured.

### Premixed Burner

The premixed burner used for the present two-phase investigations consisted of a straight-sided conical flame established at the exit of a Mache-Hebra-type nozzle [9]. A schlieren imaging system provided the flame cone angle, which was used to determine the burning velocity [11]. The nozzle exit flow profile was characterized by laser Doppler velocimeter measurements described previously [9]. The typical half-cone angle of the flame was about 20°. With addition of the solution droplets, the flame height was maintained constant at about 2.0 cm by adjusting the total flow rate of reactants while maintaining the equivalence ratio at the desired value. For the present data, the uncertainty (expanded uncertainties with a coverage factor of 2) in the burning velocity is  $\pm 6.0\%$ .

query 1

query 2

## PREMIXED AND NON-PREMIXED FLAMES WITH FINE DROPLETS OF WATER AND SOLUTIONS 3

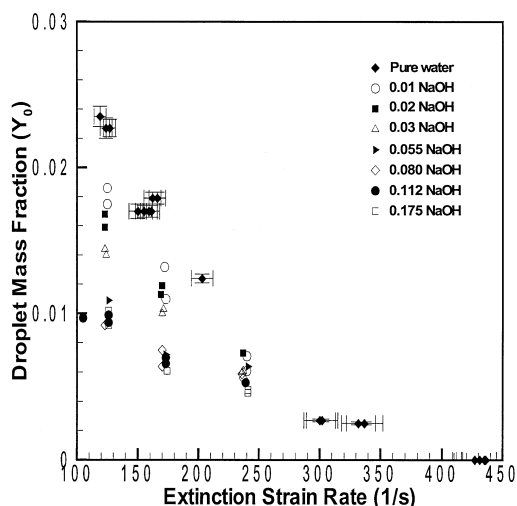


FIG. 1. Droplet mass fraction ( $Y_0$ ) as a function of extinction strain rate of a methane/air non-premixed flame for several NaOH mass fractions in water ( $y_{\text{NaOH}}$ ).

The inhibition of a laminar premixed flame can be characterized by the relative decrease in the burning velocity (denoted here by  $S_L$ ) with respect to that of an uninhibited flame ( $S_L^0$ ). The simple conical premixed flame stabilized above the Mache-Hebra nozzle, and the associated flame cone angle measurement technique adopted here is one of many traditional methods of obtaining the laminar flame speed [11]. While curvature and stretch effects do exist in the flame, they are considered minor, particularly since all results in the present work are reported as normalized flame speed,  $S_L/S_L^0$ . The uninhibited methane and air flame speed obtained from the present burner is  $35 \pm 1.2$  cm/s. Because the ultrasonic atomizer and the length of the Pyrex tube delivering the reactant gas mixture are the same as in the counterflow burner, the median droplet diameter is not expected to be different from that of the counterflow flames reported above.

#### Extinction of Non-Premixed Flames with Water Solutions

##### Water/NaOH Fine Droplets

Figure 1 shows a comparison of droplet mass fraction in air ( $Y_0$ ) as a function of the global extinction strain rate ( $a_{\text{ext}}$ ), with varying NaOH mass fraction in water ( $y_{\text{NaOH}}$ ). Similar results were reported earlier for NaOH mass fractions in water of  $y_{\text{NaOH}} = 0.055, 0.112, \text{ and } 0.175$  [6]. In the earlier data, at the lowest flow strain rate of  $125 \text{ s}^{-1}$ , the case of 0.175 NaOH in water showed a significantly higher effectiveness over 0.055 and 0.112 NaOH

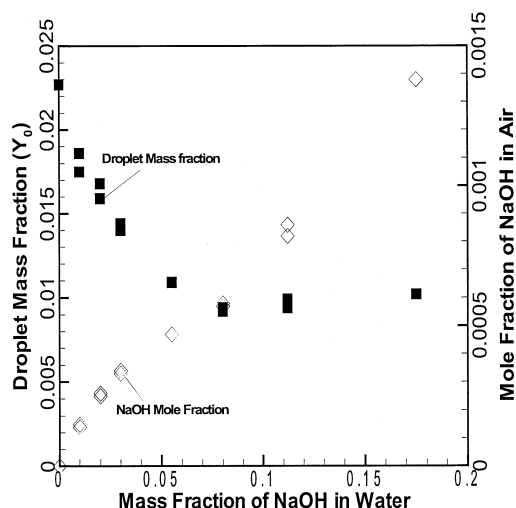


FIG. 2.  $Y_0$  and mole fraction of NaOH in air as a function of  $y_{\text{NaOH}}$  for the extinction strain of  $125 \text{ s}^{-1}$  in Fig. 1.

cases (i.e.,  $Y_0 = 0.005$  for  $y_{\text{NaOH}} = 0.175$  versus  $Y_0 = 0.010$  for  $y_{\text{NaOH}} = 0.055$  and 0.112). However, for higher extinction strain rates ( $>125 \text{ s}^{-1}$ ), the previous experimental data indicated negligible differences in extinction condition with varying NaOH mass fraction. These somewhat inconsistent results with varying NaOH mass fractions clearly required further investigation, including investigation about the effectiveness of NaOH at lower mass fractions (i.e.,  $y_{\text{NaOH}} < 0.055$ ). The new data reported here indicate that the differences in  $Y_0$  for  $y_{\text{NaOH}}$  of 0.055, 0.112, and 0.175 are within experimental uncertainty. Distinct effects of NaOH mass fraction are obtained only for  $y_{\text{NaOH}} < 0.055$ .

The difference between the new  $y_{\text{NaOH}} = 0.175$  data and previous results was found to be caused by a temperature dependence of the ultrasonic nozzle performance. When the nozzle tip was allowed to reach a steady operating temperature, typically about  $40^\circ\text{C}$  after about 15 min of continuous operation, the resulting flame extinction data were consistent and reproducible. While the revision of  $y_{\text{NaOH}} = 0.175$  data can be attributed to ultrasonic atomizer nozzle performance, the observation that the mass fraction of NaOH above 0.055 yields no apparent increase in flame suppression is rather interesting and requires further analysis.

The flame extinction results shown in Fig. 1 at the strain rate of  $125 \text{ s}^{-1}$  are replotted in Fig. 2, according to the variation of droplet mass fraction ( $Y_0$ ) versus NaOH mass fraction in water ( $y_{\text{NaOH}}$ ). As  $y_{\text{NaOH}}$  is increased above 0.08, the total droplet mass fraction ( $Y_0$ ) needed for flame extinguishment is seen to become invariant with the NaOH mass fraction in the droplet. Similar saturation behavior has

4

PART TITLE

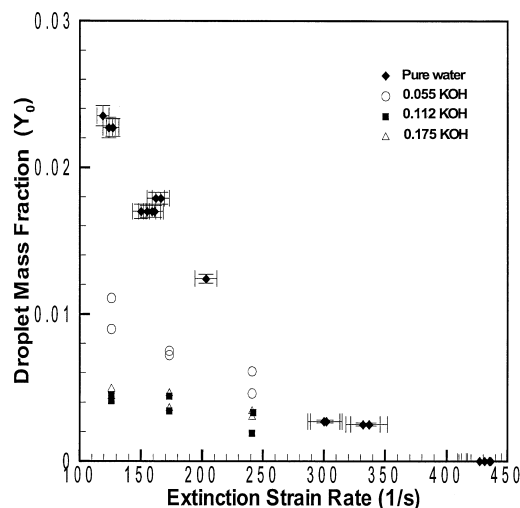


FIG. 3. Droplet mass fraction ( $Y_0$ ) as a function of extinction strain rate of a methane/air non-premixed flame for several KOH mass fractions in water ( $y_{\text{KOH}}$ ).

been reported in premixed flames with iron, manganese, and tin organometallic compounds [12,13] and metal salts added as particles [14]. Also shown in Fig. 2 is the mole fraction of NaOH in air ( $X_{\text{NaOH}}$ ), assuming that NaOH in droplets is completely released to the gas phase. Under such an assumption (reasonable if the droplets are completely vaporized at or before the flame), it is not surprising that  $X_{\text{NaOH}}$  increases almost linearly with increasing NaOH mass fraction in water/NaOH solution. In reality, however, the maximum  $X_{\text{NaOH}}$  is directly related to the partial pressure of NaOH (or any other low vapor pressure sodium compound) and is a function of temperature only. Fig. 2 indicates that this limiting value of  $X_{\text{NaOH}}$  is about 0.0006 (or 600 ppm of NaOH in air). Therefore, as seen in Fig. 2, any increase in NaOH vapor above this partial pressure, for example  $y_{\text{NaOH}} > 0.08$ , may not yield any improvement in the fire suppression ability of water/NaOH solution.

The thermochemical data of NaOH can be used to estimate the gas-phase conditions that yield limiting  $X_{\text{NaOH}} = 0.0006$ . Assuming that NaOH exists as a monomer in the gas phase, an equilibrium liquid-vapor calculation based on the Clausius-Clapeyron equation yields an NaOH saturation temperature of 1125 K [15]. This vapor-liquid equilibrium temperature is about 400–500 K below the characteristic temperature within the rate-limiting oxygen-consumption, radical-production region of the flame [16]. Because of the thermal boundary layer surrounding each evaporating droplet, it is conceivable that an effective temperature below the flame temperature may control the saturation of excess NaOH vapor. Alternatively, loss of active inhibiting species

to condensation may be controlled by a compound with a lower vapor pressure than NaOH. In experiments, resolving the appropriate effective temperature that controls saturation of condensation of the relevant species is perhaps impossible, and therefore, only detailed numerical simulations can provide better understanding of the saturation phenomenon occurring. Although numerical simulations that include detailed interactions between the condensed phase and the gas phase have recently been developed to describe water droplet interactions [17], analytical models for droplet evaporation of binary mixtures in flames have not. In this case, the modeling evaporation of binary liquid droplets with highly disparate boiling temperatures (373 K for water vs. 1663 K for NaOH) may require further simplifications. Hence, in this paper, only experimental results are presented.

#### Water/KOH Fine Droplets

Besides NaOH, other alkali-metal compounds are known to be chemically effective fire suppressants. In particular, potassium-containing compounds are believed to be more effective than sodium [14,18]. Fig. 3 shows experimentally obtained extinction strain rates of a methane/air non-premixed flame, with similar sized water/KOH droplets, containing varying mass fractions of KOH. For the lowest extinction strain rate considered (i.e.,  $125 \text{ s}^{-1}$ ), the data show increasing flame suppression up to about  $y_{\text{KOH}} = 0.112$ . Further increase in KOH mass fraction in water up to 0.175, however, yields no further increase in the flame suppression ability of the water/KOH solution. Following the analysis of water/NaOH saturation vapor conditions, current water/KOH results indicate that the KOH saturates at a gas-phase mole fraction of about  $X_{\text{KOH}} = 0.0003$  for  $y_{\text{KOH}} = 0.112$ . Liquid-vapor equilibrium data for KOH indicate that this mole fraction corresponds to a gas temperature of about 1025 K, which is about 100 K lower than that obtained for the NaOH case. This lower effective saturation temperature for KOH is consistent with the lower boiling temperature of KOH (1597 K) compared to that of NaOH (1663 K).

#### Water/NaCl and Water/ $\text{FeCl}_2$ Fine Droplets

Non-premixed methane/air flame extinction experiments were also conducted with NaCl. Water/NaCl droplets have been considered previously by Zheng et al. [5], but only in the context of extinction of counterflow premixed flames as a function of fuel-air equivalence ratio. The flame suppression trends shown in Fig. 4, with increasing NaCl mass fraction in water, are consistent with previous data with NaOH and KOH.

## PREMIXED AND NON-PREMIXED FLAMES WITH FINE DROPLETS OF WATER AND SOLUTIONS 5

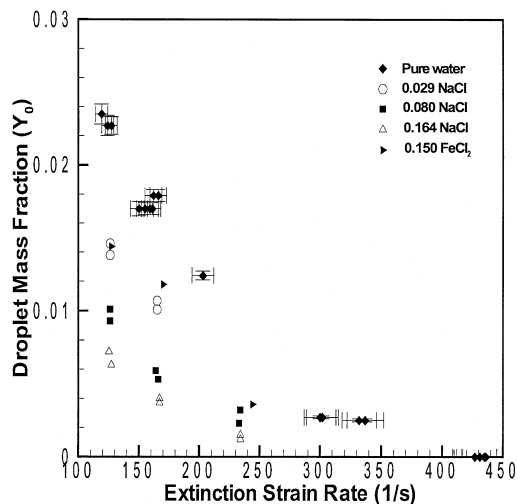


FIG. 4. Droplet mass fraction ( $Y_0$ ) as a function of extinction strain rate of a methane/air non-premixed flame for several NaCl and  $\text{FeCl}_2$  mass fractions in water ( $y_{\text{add}}$ ).

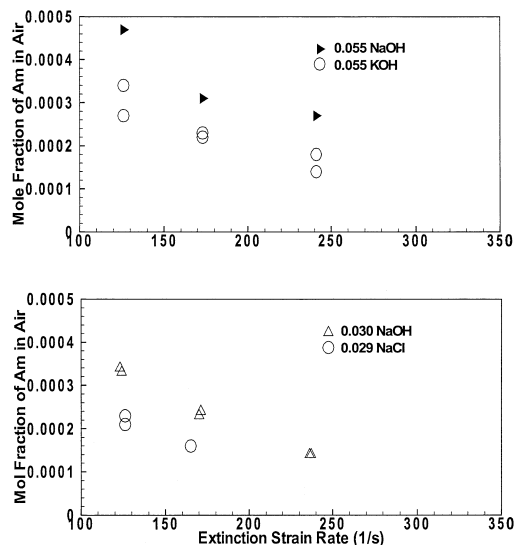


FIG. 5. Upper panel: Mole fraction of alkali metal ( $A_m$ ) in air as a function of non-premixed methane/air flame extinction strain rate for NaOH and KOH mass fractions of 0.055 shown in Figs. 2 and 4. Lower panel: Mole fraction of  $A_m$  in air as a function of non-premixed methane/air flame extinction strain rate for NaOH and NaCl mass fractions of 0.03 shown in Figs. 2 and 5 (upper panel).

The metal Fe (in  $\text{Fe}^+$  or  $\text{Fe}^{2+}$  form) has previously been shown to be very effective [7]. Here, explorative experiments were conducted to test the efficacy of  $\text{Fe}^{2+}$  compound dissolved in water. An  $\text{FeCl}_2$  mass fraction of  $y_{\text{FeCl}_2} = 0.15$  in water was tested, and this water/ $\text{FeCl}_2$  solution clearly indicates a chemical inhibition effect, as seen in Fig. 4. Although it appears that  $\text{FeCl}_2$  is not as effective as NaCl on a mass basis, experiments with lower mass fractions of  $\text{FeCl}_2$  must be performed to evaluate the occurrence of saturation phenomenon, as observed in water/NaOH solutions.

#### Molar Comparisons of NaOH, KOH, and NaCl

In order to relate the chemical inhibition of the agents considered here to previous studies, the non-premixed flame extinction results are analyzed here on a molar basis for the additive. To avoid uncertainties related to saturation effects, only additive mass fractions below the saturation condition are considered here. Since water/NaOH extinction results show saturation of NaOH vapor is approached for additive mass fractions above 0.055, the molar comparisons between NaOH and KOH are performed at  $y_{\text{add}} = 0.055$ . For the extinction data points considered, the mole fraction of alkali metal hydroxide ( $A_m\text{OH}$ ) was evaluated and is plotted as a function of flame extinction strain rate, as shown in the upper panel of Fig. 5. These molar comparisons clearly indicate roughly 2 times performance benefit of KOH over NaOH as an additive to water droplets, similar to what has been reported based on flames inhibited with particulates [14,18]. More recent kinetic studies have indicated that recombination of K with OH is about 30% faster than Na with OH and that recombination of K with  $\text{O}_2$  is in fact 2–3 times faster than Na with  $\text{O}_2$  [19], and this, perhaps, is the primary reason for the effective flame suppression by KOH.

Comparison of molar plots of NaCl versus NaOH, shown in the lower panel of Fig. 5, indicate a surprisingly superior flame suppression ability of NaCl. This is, however, consistent with the saturation of NaCl or NaOH, since the vapor pressure of NaCl at 1125 K is 1.8 times that of NaOH.

For a droplet mass loading of  $Y_0 = 0.014$  and an extinction strain rate of  $125 \text{ s}^{-1}$ , a comparison of the mole fraction of chemical agent needed in air ( $X_i$ ) yields the following order:  $X_{\text{KOH}} = 0.00021 < X_{\text{NaCl}} = 0.00023 < X_{\text{NaOH}} = 0.00034 < X_{\text{FeCl}_2} = 0.00056$  (assuming linear interpolation between available data). These values indicate that on a molar basis KOH is the most effective chemical agent, followed by NaCl and NaOH. For water/ $\text{FeCl}_2$ , the interpolation was performed assuming that  $y_{\text{FeCl}_2} = 0.15$  is unsaturated at this rather high molar loading, which is certainly questionable. If  $\text{FeCl}_2$  is found to condense at a lower additive mass fraction (e.g.,

6

PART TITLE

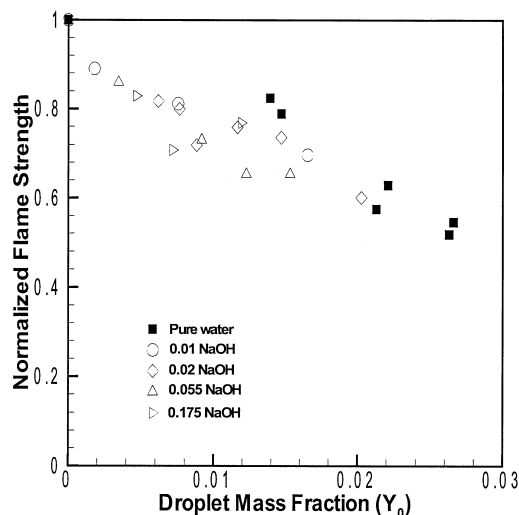


FIG. 6. Square of the normalized burning velocity of a premixed flame inhibited with fine droplets of water solution for several NaOH mass fractions in water.

$y_{\text{FeCl}_2} < 0.05$ ), then on a molar basis water/ $\text{FeCl}_2$  can become the most effective solution as  $X_{\text{FeCl}_2}$  will approach 0.00018 (instead of 0.00056 above).

#### Inhibition of Premixed Flames with Water/NaOH Droplets

The inhibition of premixed flame propagation with various chemical fire-suppressing agents is well documented [12,20,21]. Here, we consider the inhibition of a conical premixed flame with fine water/NaOH droplets. Based on phenomenological reasoning [22], it is well known that the burning velocity is proportional to the square root of the chemical reaction rate. Consequently, we plot in Fig. 6 the square of normalized burning velocity [ $S = (S_L/S_L^0)^2$ ] versus droplet mass fraction ( $Y_0$ ) for varying NaOH mass fraction in water ( $y_{\text{NaOH}}$ ). With increasing  $y_{\text{NaOH}}$ , these results do not show any significant increase in flame inhibition compared to the inhibition with pure water droplets. This is a rather unexpected finding because of the close similarities (described below) between the premixed and non-premixed flames considered.

The insensitivity of NaOH fraction in water droplets in the premixed flame configuration can be explained by considering the droplet residence times in the flame. Because of the vast difference in the boiling temperature between water and NaOH (373 K vs. 1663 K), water is expected to evaporate first. If the flow residence time of droplets through the premixed flame is less than that through counterflow flames, a partially vaporized droplet (smaller than the initial  $13\ \mu\text{m}$  at the inflow boundary) with a much

higher concentration of NaOH will emerge. Therefore, the lack of chemical inhibition observed in the premixed experiments with water/NaOH solutions may be caused by partially vaporized droplets. To test this hypothesis, the flow residence times of droplets through premixed and non-premixed flames, inhibited with pure water droplets, are investigated below.

#### Comparison of Non-premixed and Premixed Flames with Pure Water Droplets

As described above, the premixed flame burning velocity is proportional to the square root of the overall chemical reaction rate. The non-premixed flame extinction strain rate, however, is directly proportional to the chemical reaction rate. A formal asymptotic analysis [23], assuming that the overall reaction of the form fuel + oxidizer  $\rightarrow$  products is applicable to both premixed and non-premixed flames, yields the following relationship between the burning velocity and extinction strain rate,

$$(\rho_0 S_L^0)^2 \propto \left( \frac{\rho \lambda}{c_p Z_{st}^2} \right) a_{\text{ext}}$$

where  $Z_{st}$  is the stoichiometric mixture fraction (assumed to be a small parameter),  $\lambda$  the thermal conductivity, and  $c_p$  the specific heat. Based on this relationship and assuming that the mixture fraction, transport, and thermodynamic properties are not affected by the small fraction of condensed-phase agent added [24], a direct comparison of the extinction/inhibition of non-premixed and premixed flames can be accomplished by defining normalized flame strength as

$$S = \left( \frac{S_L}{S_L^0} \right)^2 = \left( \frac{a_{\text{ext,inh}}}{a_{\text{ext,uninh}}} \right)$$

Its applicability for droplets of pure water is examined in Fig. 7, which shows the normalized flame strength for the premixed and non-premixed flames as a function of the mass fraction of water. The comparison clearly shows that the  $13\ \mu\text{m}$  median diameter droplets are not equally effective in inhibiting the premixed flame. (Note that for proper normalizations,  $S_L^0$  corresponds to a case in which the premixed methane/air stream is saturated with water vapor, and  $a_{\text{ext,uninh}}$  to a case in which the non-premixed air stream is saturated with water vapor.)

#### Effect of Flow Residence Time

The aforementioned differences between the inhibition of non-premixed and premixed flames by pure water droplets, as well as the disparate results for droplets of water/NaOH in premixed flames, can be explained based on the flow residence time associated with each flame structure and its effect on

## PREMIXED AND NON-PREMIXED FLAMES WITH FINE DROPLETS OF WATER AND SOLUTIONS 7

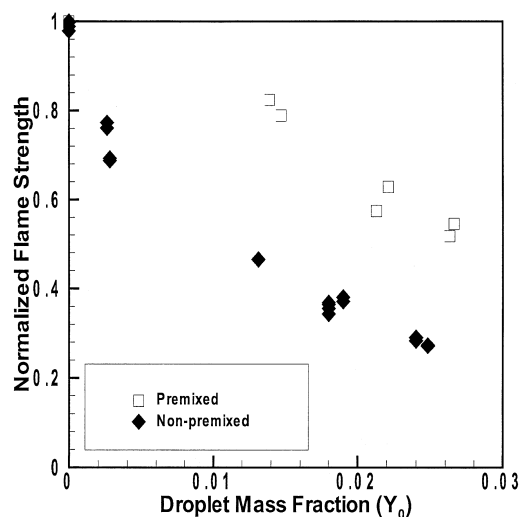


FIG. 7. Normalized flame strength of non-premixed and premixed methane/air flames inhibited with fine droplets of water with a median diameter of  $20 \mu\text{m}$ .

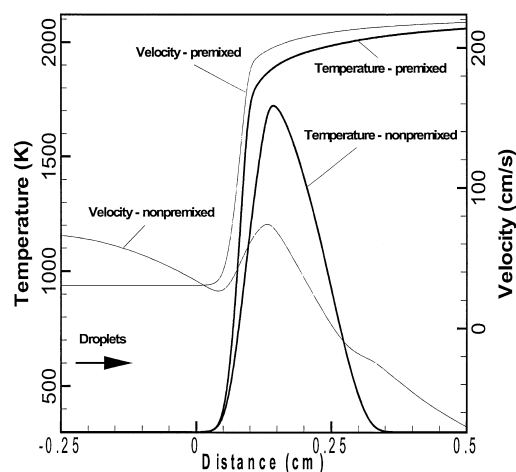


FIG. 8. Non-premixed and a premixed flame structure, corresponding to inhibited conditions of water droplet mass fraction of  $Y_0 = 0.01$ .

the evaporation of fine water droplets. Fig. 8 shows the numerically obtained flame structure of a premixed and a non-premixed flame, corresponding to conditions in which the flame is inhibited by  $13 \mu\text{m}$  droplets with a droplet mass fraction of  $Y_0 = 0.01$ . The estimated flow residence time of these droplets through the thermal layer, from the cold boundary up to the peak flame temperature, differs substantially: 4 ms for the premixed versus 14 ms for the non-premixed. This implies that the time available for the droplets to vaporize in premixed flames is considerably less and that the  $13 \mu\text{m}$  droplets are

not necessarily the ideal size for inhibiting the premixed flame considered. Consequently, the maximum thermal cooling is not achieved compared to the counterflow flame, resulting in the lower flame inhibition observed in Fig. 7 for premixed flames.

Interestingly, this finding also explains the much poorer relative effectiveness of either NaOH or KOH at  $a = 240 \text{ s}^{-1}$  versus  $a = 125 \text{ s}^{-1}$ , as shown in Figs. 1 and 3. The higher strain flames have lower residence time, possibly preventing the release of the additive to the gas phase.

### Conclusions

The low vapor pressure of alkali metals at normal room temperature requires delivery of alkali metals as a powder or as a fine-droplet spray for their efficient delivery to a flame. However, efforts to combine the thermal fire suppression ability of fine water droplets with the chemical inhibition of alkali metals have indicated the existence of an upper agent limit because of the associated limiting vapor pressure of the additive. When the mass fraction of alkali hydroxide in water is below this condensation limit, comparison of the chemical effectiveness clearly indicates that KOH is about 2 times more effective than NaOH on a molar basis for a wide range of flow strain rates. Comparison of the effectiveness of water/NaOH with water/NaCl on a molar basis indicates a superior effectiveness of NaCl over NaOH, which can be explained based on their vapor pressures.

The relationship between droplet size and flow residence time is found to be important both for comparing the behavior of condensed-phase agents between flame types, as well as for evaluating the efficacy of chemically active additives. Comparison of the effects of water/NaOH droplets on the extinction of non-premixed and inhibition of premixed flames implies that if the droplets are not completely evaporated before reaching the chemical reaction layer (because of non-optimal droplet size or too short droplet residence time), then the full chemical effectiveness of the agent is not realized. Similarly, when equally sized fine water droplets are introduced to non-premixed and premixed flames, with no velocity lag between the droplets and the gas phase, the characteristic flame extinction/inhibition conditions of the two flames differ. Flame structure analysis has revealed that the distinct flow residence time of droplets (with a median diameter of  $13 \mu\text{m}$ ) through each flame structure, that is, 14 ms for the non-premixed flame versus 4 ms for the premixed flame, is the cause for the observed differences. These results illustrate the importance of understanding the particular reacting flow field and temperature conditions in order to assess the intricate coupling between droplet size and its residence time through the flame structure.

In real fires with turbulent flow fields, the flow residence times of droplets can be very different from those in the premixed and non-premixed flames investigated here, and the optimum droplet sizes can be much larger than 10–20  $\mu\text{m}$ . Therefore, design of optimal fire-suppression systems using fine droplets of water solutions must consider the flow residence times and flame structures of each application carefully.

#### Acknowledgments

This work was supported by the DoD SERDPS's Next Generation Fire Suppression Technology Program and by NIST internal funding.

#### REFERENCES

1. Grant, G., Brenton, J., Drysdale, D., *Prog. Energy Combust. Sci.* 26:79 (2000).
2. Zegers, E. J. P., Williams, B. A., Sheinson, R. S., and Fleming, J. W., *Proc. Combust. Inst.* 28:2931 (2000).
3. Lentati, A. M., and Chelliah, H. K., *Proc. Combust. Inst.* 27:2839 (1998).
4. Prasad, K., Li, C., Kailasanath, K., Ndubizu, C., Ananth, R., and Tatem, P., *Combust. Sci. Technol.* 132:325–364 (1998).
5. Zheng, R., Bray, K. N. C., and Rogg, B., *Combust. Sci. Technol.* 126:389 (1997).
6. Lazzarini, A. M., Krauss, R. H., Chelliah, H. K., and Linteris, G. T., *Proc. Combust. Inst.* 28:2939 (2000).
7. Vanpee, M., and Shirodkar, P. P., *Proc. Combust. Inst.* 17:787 (1978).
8. Mitani, T., and Niioka, T., *Combust. Flame* 55:13 (1984).
9. Wanigarathne, P. C., M. S. thesis, University of Virginia, 2001.
10. Seshadri, K., and Williams, F. A., *Int. J. Heat Mass Transfer* 21:251 (1978).
11. Andrews, G. E., and Bradley, D., *Combust. Flame* 18:133 (1972).
12. Reinelt, D., and Linteris, G. T., *Proc. Combust. Inst.* 26:1421 (1996).
13. Linteris, G. T., Knyazev, V., and Babushok, V., *Combust. Flame.*, in press.
14. Rosser, W. A., Inami, S. H., Wise, H., *Combust. Flame* 7:107 (1963).
15. NIST Chemistry WebBook, no. 69, July 2001 release, <http://webbook.nist.gov/chemistry/>.
16. Chelliah, H. K., and Williams, F. A., *Combust. Flame* 80:17 (1990).
17. Lentati, A. M., and Chelliah, H. K., *Combust. Flame* 115:158–179 (1998).
18. Friedman, R., and Levy, J. B., *Combust. Flame* 7:195 (1963).
19. Patrick, R., and Golden, D. M., *Int. J. Chem. Kinet.* 16:1567 (1984).
20. Lask, G., Wagner, H. G., *Proc. Combust. Inst.* 8:432 (1962).
21. da Cruz, F. N., Vandooren, J., and Van Tiggelen, P., *Bull. Soc. Chim. Belg.* 97(11–12):1011–1029 (1988).
22. Williams, F. A., *Combustion Theory*, 2nd ed., Benjamin/Cummings, 1985.
23. Peters, N., *Combust. Sci. Technol.* 30:1 (1983).
24. Chelliah, H. K., Yu, G., Hahn, T. O., and Law, C. K., *Proc. Combust. Inst.* 24:1083 (1992).